Battery Dispatch Optimization for Electric Vehicle Aggregators: A Decentralized Mixed-Integer Least-Squares Approach with Disjunctive Cuts

Chao Lei, *Member, IEEE*, Y. Christine Chen, *Member, IEEE*, Siqi Bu, *Senior Member, IEEE*, Shuangqi Li, *Member, IEEE*, Qianggang Wang, *Senior Member, IEEE*, and Lalit Goel, *Fellow, IEEE*

***Abstract*—To address battery dispatch optimization (BDO) for an electric vehicle (EV) aggregator, this paper develops a decentralized mixed-integer least-squares (DMILS) approach formulated with a master-problem and multiple sub-problems based on decomposition via the alternating direction method of multipliers (ADMM) algorithm. The aggregator's master-problem aims to coordinate the Lagrange multiplier vector in all sub-problems, whilst each EV's sub-problem concentrates on its individual BDO solution using the updated Lagrange multipliers. To accelerate solution convergence, disjunctive cuts for battery operation are incorporated into the proposed DMILS approach. Given parallel computation of sub-problems and a well-designed warm-start strategy, numerical case studies demonstrate that the proposed DMILS approach converges to a solution with the same objective function value as a benchmark centralized counterpart in only several iterations, thus incurring lower computation time and minor communication overhead.**

***Index Terms*—Battery dispatch optimization, decentralized mixed-integer least-squares, disjunctive cut, EV aggregator**

I. Introduction

Electric vehicles (EVs) primarily serve the purpose of enabling mobility without tailpipe emissions, thus representing an integral component of the zero-carbon energy transition. At present, EVs can also be equipped with bidirectional vehicle-to-grid (V2G) charging capability, enabling EV owners to sell excess energy stored in their vehicle batteries back to the distribution network (DN) [1]. Aggregators interface the distribution system and end users, including distributed generation, flexible loads, battery storage, and EVs, to contribute to reliable and efficient operation of DNs. For simplicity, we assume that an aggregator coordinates only EVs with V2G contracts and performs the day-ahead battery dispatch optimization (BDO) to schedule charging and discharging power from the EVs following an aggregate signal prescribed by the distribution system operator (DSO) [2], [3].

Typically, the battery operation in the BDO problem is formulated as a mixed-integer linear programming (MILP) problem to satisfy charge-discharge complementary constraints that avoid solutions with simultaneous charging and discharging [2]. However, an aggregator generally manages a large population of EVs, leading to a large number of binary variables in the BDO model. In place of the linear objective function, a quadratic objective function in least-squares form can be adopted to track the prescribed aggregate power signals. The resultant BDO problem becomes a large-scale mixed-integer quadratic program (MIQP), the solution of which poses significant computational challenge.

In the existing literature, there are two general lines of research that address the computational challenge associated with solving the BDO problem, the first involving model approximations and the second being decentralized computation approaches. Prior work in model approximations typically employs the relaxation of binary variables. For example, the H-representation convex hull (HCH-LP) approach in [2] applies a tightened constraint to approximate the nonconvex complementary constraint while relaxing all binary variables. References [3] and [4] propose a physically realizable BDO approach without binary variables, which renders a near-optimal solution. However, approximations based in binary variable relaxation do not offer theoretical guarantees in satisfying the charge-discharge complementary constraints, and only with integer variables in the BDO problem can these constraints be strictly satisfied.

Generally speaking, decentralized solution approaches assign computational tasks across individual EVs, and as such, they are highly scalable alongside the proliferation of EVs. For example, [5] proposes a distributed coordination mechanism between EV demands and V2G-based capability is transformed into an iterative price-based coordination algorithm for aggregators, and [6] uses the Benders decomposition to optimize distribution system operation involving EV aggregators. However, the BDO model in these references is over simplified as a linear problem with relaxed binary variables, which may result in simultaneous charge-discharge solutions. The Lagrange relaxation used in [7] optimally coordinates the charging power signals in different parking decks, but it does not consider discharging actions and thus the corresponding solution does not apply to V2G-based BDO problems. Instead, decentralized approaches to address V2G-based BDO problems also include heuristic algorithms, such as the whale optimization algorithm [8] and water-filling-based algorithm [9], [10]. The whale optimization algorithm relies heavily on suitable tuning of hyperparameters. The water-filling-based algorithm requires optimal charging/discharging power objec-

This work was supported in part by the Natural Science Foundation of China under Grant 52077017.

Chao Lei and Y. Christine Chen are with the Department of Electrical and Computer Engineering, The University of British Columbia, Vancouver, Canada (e-mail: chao.lei@ubc.ca and chen@ece.ubc.ca)

Siqi Bu and Shuangqi Li are with the Department of Electrical and Electronic Engineering, The Hong Kong Polytechnic University, Hong Kong, China (e-mail: Siqi.bu@gmail.com and shuangqi.li@polyu.edu.hk)

Qianggang Wang is with State Key Laboratory of Power Transmission Equipment Technology, Chongqing University, Chongqing, China (e-mail: qianggang1987@cqu.edu.cn).

Lalit Goel is with the Department of Electrical and Electronic Engineering, Nanyang Technological University, Singapore(e-mail: elkgoel@ntu.edu.sg).

tives for different EVs, but such prior information may not be available before solving the BDO problem. Also, the relaxation of equality constraints into the Lagrangian function in the water-filling-based algorithm may result in infeasible solutions that do not satisfy the equality constraints.

Unlike aforementioned approaches, this paper addresses the computational challenge of solving the BDO problem by drawing inspiration from [11] that employs disjunctive convex hull relaxation (DCHR), albeit for the problem of distribution network reconfiguration. Similar to [11], we divide the feasibility space of the BDO problem with valid disjunctive cuts that can then reduce the search space without resorting to binary variable relaxation. Furthermore, we develop the decentralized mixed-integer least-squares (DMILS) approach based on alternating direction method of multipliers (ADMM) in conjunction with a warm-start strategy that leads to reduced computation time and convergence in only several iterations.

II. Problem Formulation and Disjunctive Cuts

In this section, we formulate the BDO problem of an EV aggregator and develop disjunctive cuts for single EV battery operation.

A. BDO Problem of an EV Aggregator

Suppose that all EVs are available over a predefined time horizon for EV aggregators with the architecture shown in Fig. 1(a). Let $\boldsymbol{P}_{c,i}^t$ and $\boldsymbol{P}_{d,i}^t$ respectively denote charging and discharging power for the i-th EV battery in time period t, and denote its state of energy (SoE) in time period t by $\boldsymbol{e}_i^t$. Further employ binary variables $\boldsymbol{\lambda}_{c,i}^t$ and $\boldsymbol{\lambda}_{d,i}^t$ to indicate whether the i-th EV is charging or discharging in time period t. Each battery i begins with initial SoE $\boldsymbol{e}_i^0$ and ends with full energy at the end of the scheduling horizon with $t = T$. Furthermore, EV batteries are scheduled to charge and discharge to collectively follow an aggregate power signal $\boldsymbol{p}_{ref}^t$ prescribed by the DSO. Then, the conventional BDO model for an EV aggregator is formulated as follows:

$$\min \ \boldsymbol{F} = \sum_{t=1}^{N_T} \left\| \sum_{i=1}^{N_E} (\boldsymbol{P}_{c,i}^t + \boldsymbol{P}_{d,i}^t) - \boldsymbol{p}_{ref}^t \right\|_2^2, \tag{1a}$$

$$\text{s.t. } \boldsymbol{e}_i^{t+1} = \boldsymbol{e}_i^t + \eta_{c,i}\boldsymbol{P}_{c,i}^t \Delta \boldsymbol{T} + \frac{1}{\eta_{d,i}} \boldsymbol{P}_{d,i}^t \Delta \boldsymbol{T}, \tag{1b}$$

$$\boldsymbol{e}_i^t = \overline{E}, \text{ if } t = T, \tag{1c}$$

$$\boldsymbol{0} \leqslant \boldsymbol{P}_{c,i}^t \leqslant \boldsymbol{\lambda}_{c,i}^t \overline{P}, \quad -\boldsymbol{\lambda}_{d,i}^t \overline{P} \leqslant \boldsymbol{P}_{d,i}^t \leqslant \boldsymbol{0}, \quad \underline{E} \leqslant \boldsymbol{e}_i^t \leqslant \overline{E}, \tag{1d}$$

$$\boldsymbol{\lambda}_{c,i}^t + \boldsymbol{\lambda}_{d,i}^t \leqslant 1, \ \boldsymbol{\lambda}_{c,i}^t, \boldsymbol{\lambda}_{d,i}^t \in \mathbb{Z}, \ \forall t \in \mathcal{T}, \ \forall i \in \mathcal{E}, \tag{1e}$$

where $\mathcal{E}$ and $\mathcal{T}$ are sets of EVs and time periods with cardinality N_E and N_T, respectively, $\Delta \boldsymbol{T}$ is the duration of each time period, e.g., $\Delta \boldsymbol{T} = 1$ for one-hour period, $\overline{P}$ denotes the charging/discharging capacity, $\overline{E}$ is the energy capacity, $\underline{E}$ is the minimum energy reserve, and $\eta_{c,i}$ and $\eta_{d,i}$ are charging and discharging efficiency coefficients, respectively [2].

B. Disjunctive Cuts for Single EV Battery Operation

The many binary variables $\boldsymbol{\lambda}_{c,i}^t$ and $\boldsymbol{\lambda}_{d,i}^t$, $i \in \mathcal{E}$, in the BDO problem pose significant challenges for fast solution convergence. In order to enhance computational performance, we introduce tightened constraints for each EV $i \in \mathcal{E}$ by noticing that the pair of indicator variables $\boldsymbol{\lambda}_{c,i}^t$ and $\boldsymbol{\lambda}_{d,i}^t$ is disjunctive,

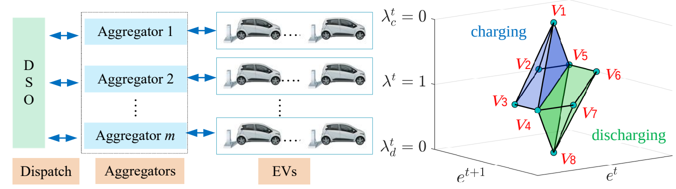

(a) (b)

Fig. 1. (a) EV aggregator architecture; (b) disjunctive closure of $\boldsymbol{\Omega}_{op}$.

and they can be used to represent the charging, discharging, and idle statuses, i.e., $(\boldsymbol{\lambda}_{c,i}^t, \boldsymbol{\lambda}_{d,i}^t) = (1, 0)$ represents charging mode; $(\boldsymbol{\lambda}_{c,i}^t, \boldsymbol{\lambda}_{d,i}^t) = (0, 1)$ refers to discharging mode; and we use $\boldsymbol{P}_{c,i}^t = \boldsymbol{P}_{d,i}^t = 0$ instead of $(\boldsymbol{\lambda}_c^t, \boldsymbol{\lambda}_d^t) = (0, 0)$ to indicate an idle state because an idle state can also exist with $(\boldsymbol{\lambda}_c^t, \boldsymbol{\lambda}_d^t) = (1, 0)$ or $(0, 1)$.

Given the disjunctive nature of battery operation, we define the disjunctive convex set $\boldsymbol{\Omega}_{op,i}$ for charging/discharging status of i-th EV battery. It includes $\boldsymbol{\Omega}_{c,i}$ and $\boldsymbol{\Omega}_{d,i}$ as the disjunctive convex sets for operational constraints (1b)–(1d) combined with $\boldsymbol{\lambda}_{c,i}^t = 1$, $\boldsymbol{\lambda}_{d,i}^t = 0$ and $\boldsymbol{\lambda}_{c,i}^t = 0$, $\boldsymbol{\lambda}_{d,i}^t = 1$. This disjunctive convex set is clearly coupled across time periods in the set $\mathcal{T}$, and we have

$$\boldsymbol{\Omega}_{op,i} = \textbf{Conv}(\boldsymbol{\Omega}_{c,i} \cup \boldsymbol{\Omega}_{d,i}), \quad \forall i \in \mathcal{E}, \tag{2a}$$

$$\boldsymbol{\Omega}_{c,i} = \{\boldsymbol{x}_i^t \in \mathbb{R} | (1\text{b}) - (1\text{d}), 0 \leqslant \boldsymbol{P}_{c,i}^t \leqslant \overline{P}, \boldsymbol{P}_{d,i}^t = 0, \forall t \in \mathcal{T}\}, \tag{2b}$$

$$\boldsymbol{\Omega}_{d,i} = \{\boldsymbol{x}_i^t \in \mathbb{R} | (1\text{b}) - (1\text{d}), -\overline{P} \leqslant \boldsymbol{P}_{d,i}^t \leqslant 0, \boldsymbol{P}_{c,i}^t = 0, \forall t \in \mathcal{T}\}. \tag{2c}$$

Depicted in Fig. 1(b) is the geometric closure of $\boldsymbol{\Omega}_{op,i}$ with continuous variation of $\boldsymbol{\lambda}_{c,i}^t$, $\boldsymbol{\lambda}_{d,i}^t \in [0, 1]$ in the $(\boldsymbol{e}^t, \boldsymbol{e}^{t+1}, \boldsymbol{\lambda}^t)$-space, where $\boldsymbol{\lambda}^t$ refers to both $\boldsymbol{\lambda}_{c,i}^t$ in the upward axis and $\boldsymbol{\lambda}_{d,i}^t$ in the downward axis, and the green and blue regions respectively represent discharging and charging feasibility spaces. The geometric closures of $\boldsymbol{\Omega}_{c,i}$ and $\boldsymbol{\Omega}_{d,i}$ are disjunctive polyhedral sets with vertices $V_1 - V_5$ and $V_4 - V_8$ in blue and green convex hulls, respectively. Note that the former vertical coordinate axis is upward with $\boldsymbol{\lambda}_{c,i}^t$ decreasing from $\boldsymbol{\lambda}_i^t = 1$ to $\boldsymbol{\lambda}_{c,i}^t = 0$, while the latter vertical axis is downward with $\boldsymbol{\lambda}_{d,i}^t$ decreasing from $\boldsymbol{\lambda}_i^t = 1$ to $\boldsymbol{\lambda}_{d,i}^t = 0$. For $\boldsymbol{\lambda}_{c,i}^t = 0$ and $\boldsymbol{\lambda}_{d,i}^t = 0$, $V_1 = (\boldsymbol{e}_i^t, \boldsymbol{e}_i^t)$ and $V_8 = (\boldsymbol{e}_i^t, \boldsymbol{e}_i^t)$. On the $(\boldsymbol{e}^t, \boldsymbol{e}^{t+1})$-plane with $\boldsymbol{\lambda}^t = 1$ (i.e., either $\boldsymbol{\lambda}_{c,i}^t = 1$ or $\boldsymbol{\lambda}_{d,i}^t = 1$), the feasibility space is a hexagon with $V_2 = (\overline{E} - \eta_{c,i}\overline{P}, \overline{E})$, $V_3 = (\boldsymbol{e}_0, \boldsymbol{e}_0 + \eta_{c,i}\overline{P})$, $V_4 = (\boldsymbol{e}_0, \boldsymbol{e}_0)$, $V_5 = (\overline{E}, \overline{E})$, $V_6 = (\overline{E}, \overline{E} - \frac{1}{\eta_{d,i}}\overline{P})$ and $V_7 = (\boldsymbol{e}_0 - \frac{1}{\eta_{d,i}}\overline{P}, \boldsymbol{e}_0)$. From the operational perspective, this hexagon represents the maximum charging/discharging between adjacent time periods. Compared with feasible set with vertices $V_1 - V_7$ constructed in [2], the disjunction described above clearly confines $\boldsymbol{\Omega}_{op,i}$ in a smaller feasibility space, i.e., in either blue or green polyhedron. Mathematically, the set of disjunctive cuts in Fig. 1(b) for $\forall i \in \mathcal{E}$ and $\forall t \in \mathcal{T}$ are expressed as follows:

$$\boldsymbol{e}_i^{t+1} \geqslant \max\{\boldsymbol{e}_{0,i} - \frac{1}{\eta_{d,i}}\overline{P}(t - 1 + \lambda_{d,i}^t)\Delta\boldsymbol{T}, \underline{E}\}, \tag{3a}$$

$$\boldsymbol{e}_i^{t+1} \leqslant \min\{\boldsymbol{e}_{0,i} + \eta_{c,i}\overline{P}(t - 1 + \lambda_{c,i}^t)\Delta\boldsymbol{T}, \overline{E}\}, \tag{3b}$$

$$\frac{1}{\eta_{d,i}}\boldsymbol{P}_{d,i}^t \Delta\boldsymbol{T} \leqslant \boldsymbol{e}_i^{t+1} - \boldsymbol{e}_i^t \leqslant \eta_{c,i}\boldsymbol{P}_{c,i}^t \Delta\boldsymbol{T}, \ \forall i \in \mathcal{E}, \tag{3c}$$

where (3c) guarantees the idle status for each EV battery, i.e., $\boldsymbol{e}_i^{t+1} = \boldsymbol{e}_i^t$ if $\boldsymbol{P}_{c,i}^t = \boldsymbol{P}_{d,i}^t = 0$.

Based on these tailored disjunctive cuts, we summarize the feasibility space for the i-th EV battery as $\mathcal{X}_i := \{\boldsymbol{x}_i^t | (1\text{b}) - (1\text{e}), (3\text{a}) – (3\text{c})\}$, where $\boldsymbol{x}_i^t := [\boldsymbol{e}_i^t, \boldsymbol{P}_{c,i}^t, \boldsymbol{P}_{d,i}^t, \boldsymbol{\lambda}_{c,i}^t, \boldsymbol{\lambda}_{d,i}^t]^T$, $i \in \mathcal{E}$

and $t \in \mathcal{T}$. This feasibility space $\mathcal{X}_i$ provides more tightened bounds than those in (1a)–(1e) alone.

III. Proposed Solution Approach

In this section, we formulate the proposed DMILS approach and introduce a warm-start strategy that contributes to fast convergence of the proposed DMILS approach.

A. DMILS Approach

In the conventional BDO problem in (1a)–(1e) with N_E EV batteries, decision variables related to different EVs are coupled only in the objective function (1a), whilst operational constraints (1b)–(1e) are separable for different EV batteries. To reduce notational burden, let $\boldsymbol{c}^T\boldsymbol{x}_i^t = \boldsymbol{P}_{c,i}^t + \boldsymbol{P}_{d,i}^t$, where $\boldsymbol{c}$ refers to a constant vector and $\boldsymbol{x}_i^t$ is previously defined as the vector of decision variables for the i-th EV battery at time t. We incorporate $\boldsymbol{p}_{sig,i}^t$ as the i-th EV's reference power signal at time t, where $i \in \mathcal{E}$. Aiming at tracking the prescribed aggregate power signal at time t, we propose the following BDO model:

$$\min\ \boldsymbol{F} = \sum_{t=1}^{N_T} \left\| \sum_{i=1}^{N_E} (\boldsymbol{c}^T\boldsymbol{x}_i^t - \boldsymbol{p}_{sig,i}^t) \right\|_2^2, \tag{4a}$$

$$\text{s.t.}\ \sum_{i=1}^{N_E} \boldsymbol{p}_{sig,i}^t = \boldsymbol{p}_{ref}^t,\ \forall t \in \mathcal{T},\ \text{and (1b)}-\text{(1e),(3a)}-\text{(3c)}. \tag{4b}$$

The triangle inequality implies that the objective function (4a) satisfies

$$\left\| \sum_{i=1}^{N_E} (\boldsymbol{c}^T\boldsymbol{x}_i^t - \boldsymbol{p}_{sig,i}^t) \right\|_2^2 \leqslant \sum_{i=1}^{N_E} \left\| \boldsymbol{c}^T\boldsymbol{x}_i^t - \boldsymbol{p}_{sig,i}^t \right\|_2^2. \tag{5}$$

Thus, the right-hand side of (5) serves as an upper bound of (4a), and the minimization of the upper bound can be used to minimize (4a), which yields the following reformulation of the BDO model in (4a)–(4b):

$$\min\ \boldsymbol{G} = \sum_{i=1}^{N_E} \boldsymbol{f}_i^t(\boldsymbol{x}_i^t),\quad \text{s.t. (4b)}, \tag{6}$$

where $\boldsymbol{f}_i^t(\boldsymbol{x}_i^t) = ||\boldsymbol{c}^T\boldsymbol{x}_i^t - \boldsymbol{p}_{sig,i}^t||_2^2$.

In (6), the objective function can be decomposed into terms pertinent to each EV. Moreover, (1b)–(1e) and (3a)–(3c) are constraints for each EV, so the only coupling constraint in (6) is the equality constraint $\sum_{i=1}^{N_E} \boldsymbol{p}_{sig,i}^t = \boldsymbol{p}_{ref}^t$. We can thus decompose the BDO problem in (6) via ADMM into individual EV sub-problems. To this end, let $\boldsymbol{\mu}^t \in \mathbb{R}^{N_T}$ denote the vector of Lagrange multipliers corresponding to the coupling constraint. By keeping the remaining constraints (1b)–(1e) implicit, the augmented Lagrangian function $\mathcal{L}$ is expressed as

$$\begin{aligned}\mathcal{L}(\boldsymbol{\mu}, \boldsymbol{p}_{sig}^t, \boldsymbol{x}^t) =& \sum_{i=1}^{N_E} \boldsymbol{f}_i^t(\boldsymbol{x}_i^t) + (\boldsymbol{\mu}^t)^T (\sum_{i=1}^{N_E} \boldsymbol{p}_{sig,i}^t - \boldsymbol{p}_{ref}^t) \\ &+ \boldsymbol{\rho}/2 || \sum_{i=1}^{N_E} \boldsymbol{p}_{sig,i}^{t,k} - \boldsymbol{p}_{ref}^t ||_2^2,\end{aligned} \tag{7}$$

where $\boldsymbol{\rho}$ is a penalty factor.

According to ADMM-based decomposition theory [12], the augmented Lagrangian function in (7) can be further divided into N_E sub-problems if Lagrange multiplier vector $\boldsymbol{\mu}^t$ is fixed. Each sub-problem represents the single battery dispatch of a particular EV, and the N_E sub-problems can be coordinated by updating the Lagrange multiplier vector $\boldsymbol{\mu}^t$ in the master problem. The i-th sub-problem calculates optimal charging/discharging profile for the i-th EV with $(\boldsymbol{x}_i^{t,k+1}, \boldsymbol{p}_{sig,i}^{t,k+1})$ at the k-th iteration, yielding

sub-problem:

$$\begin{aligned}(\boldsymbol{x}_i^{t,k+1}, \boldsymbol{p}_{sig,i}^{t,k+1}) =& \underset{\boldsymbol{x}_i^t, \boldsymbol{p}_{sig,i}^t}{\operatorname{argmin}}\ \boldsymbol{f}_i^t(\boldsymbol{x}_i^t) + (\boldsymbol{\mu}^{t,k})^T (\sum_{j=1, j\neq i}^{N_E} \boldsymbol{p}_{sig,j}^{t,k} + \boldsymbol{p}_{sig,i}^t - \boldsymbol{p}_{ref}^t) \\ &+ \boldsymbol{\rho}/2 || \sum_{j=1, j\neq i}^{N_E} \boldsymbol{p}_{sig,j}^{t,k} + \boldsymbol{p}_{sig,i}^t - \boldsymbol{p}_{ref}^t ||_2^2, \\ &\text{s.t. (1b)}-\text{(1e), (3a)}-\text{(3c)},\end{aligned} \tag{8}$$

where $\boldsymbol{\mu}^{t,k}$ and $\boldsymbol{p}_{sig,j}^{t,k}$ are solved from the master-problem and other sub-problems at the k-th iteration, respectively. Once all sub-problems are solved in parallel at the k-th iteration, the aggregator conducts bidirectional communication among all EVs by updating $\boldsymbol{\mu}^{t,k+1}$ in the master problem at k+1-th iteration.

master-problem:

$$\boldsymbol{\mu}^{t,k+1} = \boldsymbol{\mu}^{t,k} + \boldsymbol{\rho} (\sum_{i=1}^{N_E} \boldsymbol{p}_{sig,i}^{t,k+1} - \boldsymbol{p}_{ref}^t),\quad \forall t \in \mathcal{T}. \tag{9}$$

The sub-problems, each with fewer decision variables, can be solved in parallel at the same time, and the master-problem is very simple in updating the Lagrange multipliers via (9). The iterative process terminates when the total least-square errors satisfy the following stopping criteria:

$$||\boldsymbol{F}^{k+1} - \boldsymbol{F}^k||_2 \leqslant \epsilon_1,\quad ||\boldsymbol{\mu}^{t,k+1} - \boldsymbol{\mu}^{t,k}||_2 \leqslant \epsilon_2,\ \forall t \in \mathcal{T}, \tag{10}$$

where $\boldsymbol{F}^k = \sum_{t=1}^{N_T} || \sum_{i=1}^{N_E} (\boldsymbol{c}^T\boldsymbol{x}_i^{t,k} - \boldsymbol{p}_{sig,i}^{t,k}) ||_2^2$, and ϵ_1 and ϵ_2 are predetermined thresholds.

B. Warm-Start Strategy

Seeking $\boldsymbol{p}_{sig,i}^{t*}$ is crucial for reaching global optimality in the DMILS approach, and in turn suitable initial $\boldsymbol{p}_{sig,i}^{t,0}$ is essential for fast convergence of the proposed iterative approach. Thus, we utilize a warm-start strategy for the proposed DMILS approach by solving the integer-relaxed BDO model for the initial guess $\boldsymbol{p}_{sig}^{t,0}$ before iterations begin. Recall that the integer-relaxed BDO model imposes the continuous relaxation of binary variables $\boldsymbol{\lambda}_{c,i}^t$ and $\boldsymbol{\lambda}_{d,i}^t$, yielding

integer-relaxed BDO model:

$$\min\ \text{(4a)}, \tag{11a}$$

$$\text{s.t. (1b)}-\text{(1d), (3a)}-\text{(3c)}, \tag{11b}$$

$$\boldsymbol{\lambda}_{c,i}^t + \boldsymbol{\lambda}_{d,i}^t = 1, \boldsymbol{\lambda}_{c,i}^t, \boldsymbol{\lambda}_{d,i}^t \in [0,1],\ \forall t \in \mathcal{T},\ \forall i \in \mathcal{E}. \tag{11c}$$

The optimal solution $\boldsymbol{x}^{t\dagger}$ obtained from this integer-relaxed BDO model achieves the minimum objective value $\boldsymbol{F}^\dagger$ with $\boldsymbol{F}^\dagger \leqslant \boldsymbol{G}^*$, where $\boldsymbol{G}^*$ is minimum objective function value solved from the proposed BDO model in (6) corresponding to optimal solution $\boldsymbol{x}^{t*}$. Then, $\boldsymbol{x}^{t\dagger}$ may be equal to $\boldsymbol{x}^{t*}$, or another optimal solution of (6), or even infeasible for (6) with the same objective function value. For instance, suppose that

Algorithm 1 DMILS

Initialization with input $\boldsymbol{e}_0$, $\boldsymbol{\eta}_c$, $\boldsymbol{\eta}_d$, $\overline{E}$, $\underline{E}$ and $\overline{P}$ over N_E units of EV batteries and input parameters $\boldsymbol{\mu}^{t,0}$, $\boldsymbol{\rho}$, ϵ_1 and ϵ_2;
Obtain warm-start point $\boldsymbol{p}_{sig}^{t,0}$ by solving (11a)–(11c);
while $k \leqslant k_{max}$ **do**
  Each sub-problem distributively updates $(\boldsymbol{x}_i^{t,k+1}, \boldsymbol{p}_{sig,i}^{t,k+1}) \leftarrow (\boldsymbol{x}_i^{t,k}, \boldsymbol{p}_{sig,i}^{t,k})$ by solving (8) ;
  Each sub-problem distributively sends $\boldsymbol{p}_{sig,i}^{t,k+1}$ to the master-problem;
  Master-problem updates $\boldsymbol{\mu}^{t,k+1} \leftarrow \boldsymbol{\mu}^{t,k}$ by (9) and returns $\boldsymbol{\mu}^{t,k+1}$ to all sub-problems;
  if stopping condition (10) is satisfied **then**
    return optimal solution $\boldsymbol{x}_i^{t*}$ for all EV batteries;
  else
    $k \leftarrow k+1$;
  end if
end while

two batteries A and B, both with the same initial energy $\boldsymbol{e}_{0,A} = \boldsymbol{e}_{0,B}$, are scheduled over two time periods ($N_T = 2$), and $p_{ref}^t = e^*$ at time $t = 1$. An optimal solution at time $t = 1$ is $(\boldsymbol{\lambda}_{c,A}^{t*}, \boldsymbol{\lambda}_{d,A}^{t*}) = (1,0)$, $(\boldsymbol{\lambda}_{c,B}^{t*}, \boldsymbol{\lambda}_{d,B}^{t*}) = (0,0)$ and $(\boldsymbol{P}_{c,A}^{t*}, \boldsymbol{P}_{d,A}^{t*}) = (e^*, 0)$, $(\boldsymbol{P}_{c,B}^{t*}, \boldsymbol{P}_{d,B}^{t*}) = (0,0)$ with the minimum objective function value $\boldsymbol{G}^*$. However, the optimal solution of the integer-relaxed BDO model $\boldsymbol{x}^{t\dagger}$, may have three outcomes: (*i*) $\boldsymbol{x}^{t\dagger}$ is exactly equal to the optimizer yielded by solving (6), (*ii*) $\boldsymbol{x}^{t\dagger}$ is infeasible for (6) with $\boldsymbol{P}_{c,A}^{t\dagger}, \boldsymbol{P}_{d,A}^{t\dagger}, \boldsymbol{P}_{c,B}^{t\dagger}$ and $\boldsymbol{P}_{d,B}^{t\dagger}$ in $\boldsymbol{x}^{t\dagger}$ simultaneously charging and discharging, (*iii*) $\boldsymbol{x}^{t\dagger}$ is another optimal solution of (6) with, e.g., $(\boldsymbol{\lambda}_{c,A}^{t\dagger}, \boldsymbol{\lambda}_{d,A}^{t\dagger}) = (0,0)$, $(\boldsymbol{\lambda}_{c,B}^{t\dagger}, \boldsymbol{\lambda}_{d,B}^{t\dagger}) = (1,0)$ and $(\boldsymbol{P}_{c,A}^{t\dagger}, \boldsymbol{P}_{d,A}^{t\dagger}) = (0,0)$, $(\boldsymbol{P}_{c,B}^{t\dagger}, \boldsymbol{P}_{d,B}^{t\dagger}) = (e^{\dagger}, 0)$ at time $t = 1$, and all three achieve the objective function value $\boldsymbol{F}^{\dagger} = \boldsymbol{G}^*$.

This toy example illustrates two conclusions. First, the BDO model (6) may have multiple optimal solutions yielding the same objective function value $\boldsymbol{G}^*$. As the MIQP-based BDO model (4a)–(4b) differs from the upper-boundary BDO model (6) only in the objective function, the MIQP-based BDO model also may have multiple optimal solutions. Second, the integer-relaxed BDO model (11a)–(11c) can provide the optimal point $\boldsymbol{p}_{sig,i}^{t,\dagger}$ that can be used to initialize $\boldsymbol{p}_{sig,i}^{t,0}$. A near-optimal initial point $\boldsymbol{p}_{sig,i}^{t,0}$ enables the proposed DMILS approach to converge quickly. Moreover, having the warm start leads to fewer switches between charging and discharging actions. This is because $\{\boldsymbol{p}_{sig,i}^{t,0}\} \geqslant 0$ enables all EVs to run in charging mode as long as $\boldsymbol{p}_{ref}^t \geqslant 0$, whilst $\{\boldsymbol{p}_{sig,i}^{t,0}\} \leqslant 0$ leads to all EVs being in discharging mode if $\boldsymbol{p}_{ref}^t \leqslant 0$. This means that $\boldsymbol{p}_{sig,i}^{t,0}$ enables all EVs to charge/discharge at the same time, thus in fewer switching actions. With this warm-start strategy, we summarize steps in the proposed iterative approach in **Algorithm 1** with the maximum iteration number k_{max}.

IV. Case Studies

We randomly select initial SoEs of EV batteries for an EV aggregator under different given reference power signal vectors over a 24-hour scheduling horizon. Parameters of each EV battery $i \in \mathcal{E}$ are $\eta_{c,i} = 0.9$, $\eta_{d,i} = 0.95$, $\underline{E} = 0.2$, $\overline{E} = 1.0$, $\overline{\boldsymbol{P}} = 0.2$ p.u., $\boldsymbol{\rho} = 10$, and ϵ_1 and ϵ_2 are set as 0.01.

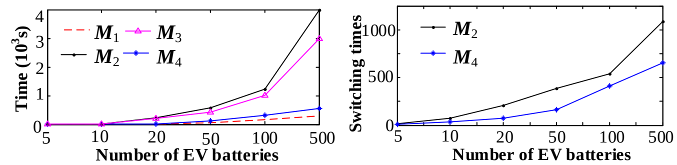

(a) (b)

Fig. 2. Computational performance w.r.t. numbers of EV batteries: (a) CPU time; (b) number of charge-discharge switches.

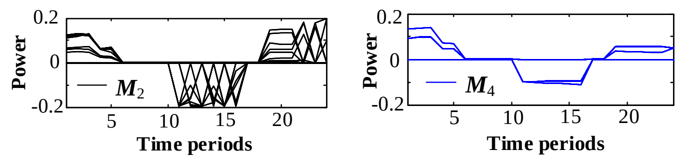

(a) (b)

Fig. 3. Optimal charge-discharge power solution: (a)$\boldsymbol{M}_2$; (b)$\boldsymbol{M}_4$.

A. Comparing with Centralized Methods

We compare the proposed DMILS approach ($\boldsymbol{M_4}$) to three centralized solution methods, the LP-based approach in [2] ($\boldsymbol{M_1}$), the MIQP-based BDO model solved using commercial solver MOSEK ($\boldsymbol{M_2}$), and the MIQP-based BDO model with disjunctive cuts solved using MOSEK ($\boldsymbol{M_3}$). Fig. 2(a) reports the computation time with respect to the numbers of EV batteries, and Fig. 2(b) plots the total number of charge-discharge switches during 24 hours for $\boldsymbol{M_2}$ and $\boldsymbol{M_4}$.

The optimal solutions of $\boldsymbol{M_1}$–$\boldsymbol{M_3}$ are achieved with the objective function value $\boldsymbol{F}^* = 0.042$ and $\boldsymbol{M_4}$ is very close with minimum objective function value $\boldsymbol{F}^* = 0.043$. As shown in Fig. 2(a), $\boldsymbol{M_1}$ incurs the least computational time because $\boldsymbol{M_1}$ is free of binary variables, but it can result in infeasible solutions featuring simultaneous charging and discharging. Otherwise, $\boldsymbol{M_4}$ is superior to both $\boldsymbol{M_2}$ and $\boldsymbol{M_3}$ with respect to computational time. In fact, for the case with $N_E = 500$ EVs (the rightmost data points in Fig. 2(a)), $\boldsymbol{M_4}$ converges to the optimal solution in 14.00% and 18.67% of the time taken by $\boldsymbol{M_2}$ and $\boldsymbol{M_3}$, respectively. Moreover, as shown in Fig. 2(b), $\boldsymbol{M_4}$ results in fewer charging/discharging switches than $\boldsymbol{M_2}$. For $\boldsymbol{M_4}$, the fewer charging/discharging switches is a side benefit of the proposed warm-start strategy. To further demonstrate the numbers of charging/discharging switches in $\boldsymbol{M_2}$ and $\boldsymbol{M_4}$, Figs. 3(a) and 3(b) present the specific optimal charge-discharge power solutions for the case with $N_E = 10$ EVs. In Fig. 3(a), $\boldsymbol{M_2}$ incurs many charging and discharging actions over 24 hours, while $\boldsymbol{M_4}$ imposes few charging and discharging actions, as shown in Fig. 3(b). This is highly beneficial as charging/discharging switches degrade the remaining useful life of EV batteries [13].

B. Comparing with Decentralized Algorithms

We implement the decentralized whale optimization algorithm ($\boldsymbol{M_5}$) [8] and water-filling based algorithm ($\boldsymbol{M_6}$) [10] for comparison with the proposed method ($\boldsymbol{M_4}$). Other parameters can be found in [8] and [9]. We assume the scheduling horizon is defined from 08:00a.m. to 07:00a.m. on th next day for the case with $N_E = 10$ EVs, and thus the discharging and charging periods in $\boldsymbol{M_6}$ are 08:00–17:00 and 18:00–07:00 on the next day, respectively. Fig. 4(a) plots the minimum objective function values in every time period

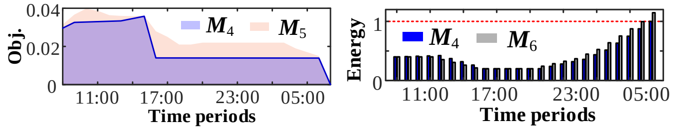

(a) (b)

Fig. 4. (a) Minimum objective function values in each time period; (b) optimal energy of the first EV battery.

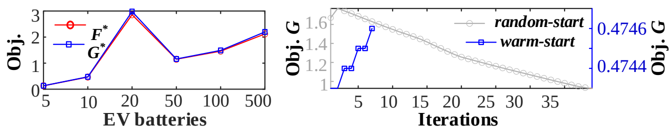

(a) (b)

Fig. 5. (a) Optimal objective function values; (b) convergence under warm-start and random-start.

for $\boldsymbol{M_4}$ and $\boldsymbol{M_5}$, indicating that $\boldsymbol{M_4}$ achieves lower values than $\boldsymbol{M_5}$, which suffers from improper hyperparameter tuning. Fig. 4(b) compares the SoE of the first EV battery over 24 hours resulting from $\boldsymbol{M_4}$ and $\boldsymbol{M_6}$. The relaxation of the SoE equality in $\boldsymbol{M_6}$ results in $\boldsymbol{e}^t \neq 1$ in the last time period.

C. Comparing with Random-Start Initialization

In Fig. 5(a), we plot the minimum objective function value $\boldsymbol{F}^*$ obtained from the benchmark $\boldsymbol{M_2}$ and compare it to $\boldsymbol{G}^*$ obtained from the proposed $\boldsymbol{M_4}$ for different numbers of EVs. We observe that, indeed, $\boldsymbol{G}^* \approx \boldsymbol{F}^*$ in all cases. Furthermore, in Fig. 5(b), for the case with $N_E = 10$ EVs, we show the convergence of the objective function $\boldsymbol{G}^*$ values resulting from $\boldsymbol{M_4}$ (under warm-start strategy) in blue-colored right y-axis and from the same but with a random-start initialization in grey-colored left y-axis. The warm-start strategy results in much faster convergence in 7 iterations to the optimal objective function value $\boldsymbol{G}^* = 0.4746$. Since we know that $\boldsymbol{F}^\dagger \leqslant \boldsymbol{F}^* \leqslant \boldsymbol{G}^*$, the objective function value $\boldsymbol{G}$ begins at $\boldsymbol{F}^\dagger$ and increases to $\boldsymbol{G}^*$ over iterations. By comparison, the random-start counterpart results in the objective function value decreasing from 1.6213 to 0.9268, much larger and with many more iterations.

D. Comparing with Integer-Relaxed BDO Model

We demonstrate that the proposed DMILS approach ($\boldsymbol{M_4}$) can indeed converge to an optimal solution from the warm-start initialization point solved from the integer-relaxed BDO model. Fig. 6(a) plots the optimal charge and discharge power solutions from $\boldsymbol{M_4}$ in blue color and from the integer-relaxed BDO model in grey color for each EV for the case with $N_E = 10$ EVs. Fig. 6(b) displays their corresponding differences in $\boldsymbol{p}_{sig,1}^{t,0}$ and $\boldsymbol{p}_{sig,1}^{t*}$ for the first EV. As demonstrated by the black and blue traces in Fig. 6(a), $\boldsymbol{M_4}$ corrects the simultaneous charging and discharging power solution that occurs in the last time period from the solution of the integer-relaxed BDO model. Correspondingly, Fig. 6(b) presents the power reference signals for one EV battery resulting from the solutions of the proposed $\boldsymbol{M_4}$ (blue trace) with warm-start initialization point solved from the integer-relaxed BDO model (black trace).

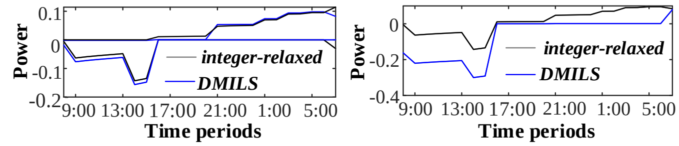

(a) (b)

Fig. 6. Comparison between DMILS and Integer-relaxed BDO model: (a) optimal charge-discharge solutions; (b) optimal $\boldsymbol{p}_{sig,i}^{t*}$ and $\boldsymbol{p}_{sig,i}^{t,0}$.

V. Concluding Remarks

In this paper, we proposed a DMILS approach combining disjunctive cuts to solve large-scale BDO problems for EV aggregators with lower computational time, optimal charge-discharge solutions with fewer switches, and minor communication overhead. Moreover, the proposed DMILS approach serves to correct the potentially infeasible solution from the integer-relaxed BDO model in only several iterations. Case studies show that the proposed DMILS approach converges to the optimal solution in 14.00% of the time taken by the benchmark centralized counterpart for the case of $N = 500$ EVs; and it achieves the optimal charge-discharge solutions with fewer charge-discharge switches than those resulting from existing methods.

References

[1] Wolinetz, A. Michael, P. Jonn, C. Jotham, and N. D. Curran, "Simulating the value of electric-vehicle–grid integration using a behaviourally realistic model," *Nat. Energy*, vol. 3, pp. 132–139, 2018.

[2] D. Pozo, "Convex hull formulations for linear modeling of energy storage systems," *IEEE Trans. on Power Syst.*, vol. 38, no. 6, pp. 5934–5936, 2023.

[3] N. Nazir and M. Almassalkhi, "Guaranteeing a physically realizable battery dispatch without charge-discharge complementarity constraints," *IEEE Trans. on Smart Grid*, vol. 14, no. 3, pp. 2473–2476, 2023.

[4] J. M. Arroyo, L. Baringo, A. Baringo, R. Bolaños, N. Alguacil, and N. G. Cobos, "On the use of a convex model for bulk storage in mip-based power system operation and planning," *IEEE Trans. on Power Syst.*, vol. 35, no. 6, pp. 4964–4967, 2020.

[5] E. L. Karfopoulos, K. A. Panourgias, and N. D. Hatziargyriou, "Distributed coordination of electric vehicles providing v2g regulation services," *IEEE Trans. on Power Syst.*, vol. 31, no. 4, pp. 2834–2846, 2016.

[6] C. Shao, X. Wang, X. Wang, C. Du, and B. Wang, "Hierarchical charge control of large populations of evs," *IEEE Trans. on Smart Grid*, vol. 7, no. 2, pp. 1147–1155, 2016.

[7] W. Qi, Z. Xu, Z.-J. M. Shen, Z. Hu, and Y. Song, "Hierarchical coordinated control of plug-in electric vehicles charging in multifamily dwellings," *IEEE Trans. on Smart Grid*, vol. 5, no. 3, pp. 1465–1474, 2014.

[8] Y. Gu and M. Liu, "Fair and privacy-aware ev discharging strategy using decentralized whale optimization algorithm for minimizing cost of evs and the ev aggregator," *IEEE Systems J.*, vol. 15, no. 4, pp. 5571–5582, 2021.

[9] H. Xing, M. Fu, Z. Lin, and Y. Mou, "Decentralized optimal scheduling for charging and discharging of plug-in electric vehicles in smart grids," *IEEE Trans. on Power Syst.*, vol. 31, no. 5, pp. 4118–4127, 2016.

[10] N. I. Nimalsiri, E. L. Ratnam, D. B. Smith, C. P. Mediwaththe, and S. K. Halgamuge, "Coordinated charge and discharge scheduling of electric vehicles for load curve shaping," *IEEE Trans. on Intell. Transport. Syst.*, vol. 23, no. 7, pp. 7653–7665, 2022.

[11] C. Lei, S. Bu, J. Zhong, Q. Chen, and Q. Wang, "Distribution network reconfiguration: A disjunctive convex hull approach," *IEEE Trans. on Power Syst.*, vol. 38, no. 6, pp. 5926–5929, 2023.

[12] S. Boyd, N. Parikh, E. Chu, B. Peleato, and J. Eckstein, *Distributed Optimization and Statistical Learning via the Alternating Direction Method of Multipliers*. Now Foundations and Trends, 2011.

[13] Y. Shi, B. Xu, Y. Tan, D. Kirschen, and B. Zhang, "Optimal battery control under cycle aging mechanisms in pay for performance settings," *IEEE Trans. on Automatic Control*, vol. 64, no. 6, pp. 2324–2339, 2019.